

Dependence of magnetoresistive properties in $[\text{Co}_{98}\text{Zr}_2 (25\text{\AA})/\text{Cu}/\text{Co} (25\text{\AA})]$ magnetic sandwiches on the Cu deposition pressure: Correlation of the “CoZrCu” disordered phase concentration and the interfacial mixed zone thickness with the Cu pressure

M. Faris^{1,*}, M. EL Harfaoui¹, A. Qachaou¹, J. Ben Youssef², H. Le Gall² and D. Meziane. Mtalsi¹

¹ *Laboratoire de Physique de la Matière Condensée (LPMC) B.P. 133-14000 Kénitra-Morocco*

² *CNRS, LPS, Groupe de Magnétisme, 92 195 Meudon, France*

The magnetoresistance (MR) and the saturation resistivity (ρ_s) are studied versus the Cu deposition pressure (P_{Cu}) at room temperature, in $[\text{Co}_{98}\text{Zr}_2 (25\text{\AA})/\text{Cu} (t_{\text{Cu}})/\text{Co} (25\text{\AA})]$ magnetic sandwiches prepared by RF diode sputtering. Results of low angle X-Ray Diffraction patterns have been proved the importante interfacial degradation observed in (CoZr/Cu) multilayers, compared to the usual (Co/Cu) structures. The highest value of transverse MR is obtained along the easy axis, and the MR curve saturates in a small magnetic field of 100 Oe at room temperature. Which leads to an interesting increase in MR sensitivity about 2%/Oe. The main features of the magnetoresistive properties evolution with Cu deposition pressure are: The maximum of MR increases and moves towards larger Cu thicknesses (t_{Cu}) for increasing P_{Cu} . The saturation resistivity ρ_s decreases with increasing t_{Cu} while it increases versus P_{Cu} . The satisfactory agreement between our experimental results and calculated ones in the framework of the Johnson-Camley semi-classical model, allows us to interpret the MR and ρ_s behavior as a result of a reinforcement of the disordered phase “CoZrCu” inside the mixed zone whose thickness t_{mx} increases with P_{Cu} .

I. INTRODUCTION

Since the discovery of giant magnetoresistance (GMR) in Fe/Cr multilayers by Baibich et al. in 1989¹, many systems have been tested and have proved the GMR effect. Thus, the Co/Cu system exhibits, at room temperature, a substantial GMR², while other systems such as Co/Cr³ and Fe/Cu⁴ present a small effect. Many authors have made great steps towards understanding the fundamental physics of this phenomenon. They have studied the magnitude of the magnetoresistance as a function of the layer thickness^{5,6}, interface morphology^{7,8}, temperature^{9,10}, configuration of the magnetic moments in the layers¹¹ and impurity scattering^{8,12}. Recently, the technology of ultrasensitive sensors allowing to increase the information storage density, requires materials with strong magnetoresistance sensitivity, $S = \Delta\text{MR}/\Delta H$, like soft materials: NiFe¹³, NiFeCo¹⁴ and FeCoB^{15,16}. The CoZr alloy presents ultrasoft properties (compared to NiFe¹⁷), which explain the great interest in increasing more and more its magnetoresistance sensitivity.

In this study we present first some experimental results of the magnetization and MR hysteresis loops measured on the $[\text{Co}_{98}\text{Zr}_2 (25\text{\AA})/\text{Cu} (28\text{\AA})/\text{Co} (25\text{\AA})]$ magnetic sandwich. This will be followed by a comparative study, based on the analysis of the XRD spectra at low angles, of (CoZr/Cu) and (Co/Cu) multilayers and of hybrid structures (Co/CoZr/Cu/CoZr/Co) and (CoZr/Co/Cu/Co/CoZr) formed by CoZr and Co interfacial insertions in (Co/Cu) and (CoZr/Cu) multilayers. Then, we examine the effect of gas pressure during Cu sputtering (P_{Cu}) on the magnetoresistive properties of the $[\text{Co}_{98}\text{Zr}_2 (25\text{\AA})/\text{Cu} (t_{\text{Cu}})/\text{Co} (25\text{\AA})]$ magnetic sandwiches, and we describe (paragraph III) the MR and ρ_s experimental results measured at room temperature. The semi-classical

approach, based on the Johnson-Camley model¹², already used in our previous study of the MR and ρ_s behavior as a function of the CoZr layer thickness (t_{CoZr}) in the $[\text{Co}_{98}\text{Zr}_2 (t_{\text{CoZr}})/\text{Cu} (28\text{\AA})/\text{Co} (25\text{\AA})]$ magnetic sandwiches⁸ is reviewed in this paper as well. In the last paragraph, we discuss the P_{Cu} effect on the magnetoresistance as function of the four specific parameters of the CoZr/Cu interface such as: the disordered phase concentration, electronic mean free path (MFP) $\bar{\ell}_{\text{mx}}$, spin-dependent scattering asymmetry (SDSA) coefficient \bar{a}_{mx}^0 and the interfacial mixed zone thickness t_{mx} . It is worth indicating that the P_{Cu} effect reinforces the interfacial disorder, accompanied by a widening of the mixed zone.

II. EXPERIMENTAL

(CoZr/Cu/Co) sandwiches were deposited on Corning 7059 glass substrates, in the presence of an in-plane DC magnetic field to induce well a defined uniaxial anisotropy. A base pressure lower than 4×10^{-7} mbar was obtained prior to the deposition in a Z550 Leybold RF diode sputtering system. A 300W RF power was applied on 10cm diameter Cu and Co targets under the constant argon pressure expected for the deposition of the Cu layers. The CoZr layer was obtained from a Co disk target covered by Zr chips (2 at% of the Zr concentration). The layer thickness was determined using a Tencor-1 profilometer, and the chemical composition of the CoZr layer was obtained from Electron Probe Microanalysis (EPMA). MR measurements were made using the four-point probe method with the current flowing in the film plane and along the induced easy-axis direction. A vibrating

sample magnetometer (VSM) was used for magnetic characterization.

III. RESULTS

A. MAGNETIZATION AND MR CURVES ANALYSIS

The magnetization versus the magnetic field (M-H) curve represented in figure 1 shows a two step process corresponding to magnetization reversal in the CoZr and Co layers at low and high fields respectively.

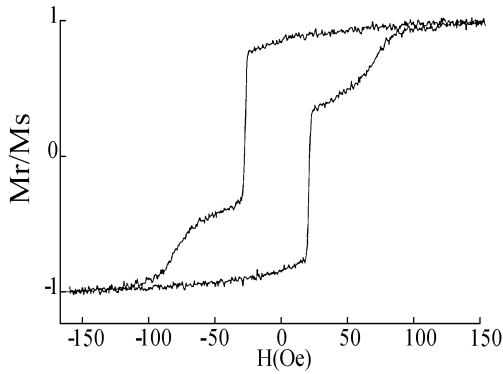


FIG. 1: M-H hysteresis loops of a $[\text{Co}_{98}\text{Zr}_2 (25\text{\AA})/\text{Cu} (28 \text{\AA})/\text{Co} (25\text{\AA})]$ sandwich.

The Co (25Å) layer compared to the CoZr (25Å) film displays a greater coercive field emphasized by a partial oxidation. The thickness of the oxidized layer was estimated to 10Å from comparative magnetization measurements of Cu/Co, Co/Cu/Co and Co/Cu systems deposited under the same conditions. The major and minor MR hysteresis loops are described in figures 2i and ii, respectively.

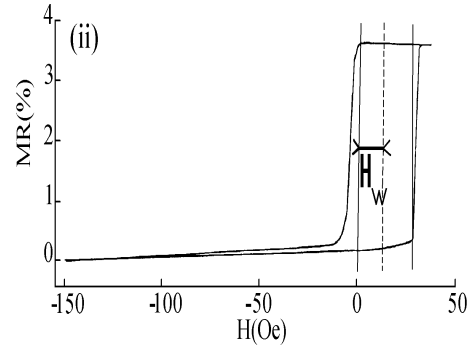
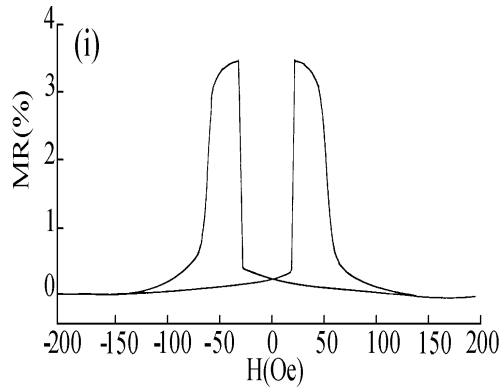


FIG. 2 : Major (i) and minor MR (ii) loops for a $[\text{Co}_{98}\text{Zr}_2 (25\text{\AA})/\text{Cu} (28 \text{\AA})/\text{Co} (25\text{\AA})]$ sandwich.

We observe that the variation of the MR versus the magnetic field presents a plateau reproducing the region in which the two magnetic layers are antiparallel. The obtained saturation field value being small, we find a good MR sensitivity which is around 2%/Oe. In contrast this sensitivity is much smaller in (Co/Cu) multilayers (about 0.02%/Oe¹⁸). Compared to usual spin-valve structures where magnetic layers are thicker ($t_{\text{mag}}=50-100\text{\AA}$), the thin layers used in our system lead to the reduction of demagnetizing field, which is desirable for applications to decrease more the size of magnetic sensors. The minor loop MR(H) associated to the CoZr layer is shown in figure 2ii, it is obtained by reversing the applied magnetic field direction when the CoZr layer is saturated. The minor loop shift compared to the major hysteresis loop allows us to deduce the bias-field H_w between the two magnetic CoZr and Co layers. The coercivity of the CoZr layer of about 17 Oe, deduced from the minor loop, is relatively large compared to values obtained in usual thick amorphous materials. This high value can be explained by an uncompletely amorphous state of the CoZr layer ((crystalline+amorphous) mixed phase¹⁹), and can thus probably be attributed to the appearance of structural defects when the CoZr magnetic layer thickness is less than a minimal value as has been pointed out in the case of NiFe thin films¹⁷.

B. XRD AT LOW ANGLES

XRD measurements at low angles have been proven to be an extremely important tool giving direct information on the structural quality of layers and interfaces. Indeed, the application of this method to CoZr/Cu films, compared to the Co/Cu films, gives us important information on the interfaces quality of these multilayers.

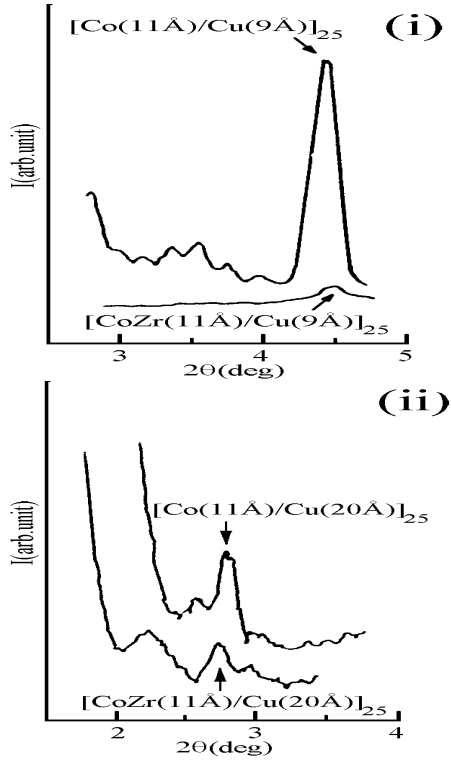


FIG. 3 : Comparative X-ray diffraction spectra at low angles of the two systems $[\text{Co}(11\text{\AA})/\text{Cu}(t_{\text{Cu}}(\text{\AA}))]_{25}$ and $[\text{Co}_{98}\text{Zr}_2 (11\text{\AA})/\text{Cu}(t_{\text{Cu}}(\text{\AA}))]_{25}$.

Comparable diffraction spectra from these two systems are represented in figures 3i and ii for a small Zr content ($x_{\text{Zr}}=2\%$), and for two Cu thicknesses ($t_{\text{Cu}}=9$ and 20\AA).

These spectra allow us to evaluate the effect of the injection of Zr impurities in Co on the structural quality of layers and interfaces.

The analysis of the first Bragg line intensity, that reflects interfaces quality, shows that for small values of Cu thicknesses ($t_{\text{Cu}} \approx 20\text{\AA}$) this intensity is weaker in (CoZr/Cu) magnetic structures than in (Co/Cu) multilayers. This indicates a strong degradation of the CoZr/Cu interface under the effect of Zr addition for small values of t_{Cu} and could be related to the existence of a disordered phase which appears for small t_{Cu} .

To better understand the effect of Zr injection in interfaces, we have also represented in figures 4i and ii the XRD spectra corresponding to the interfacial insertions of CoZr and Co films in (Co/Cu) and (CoZr/Cu) multilayers.

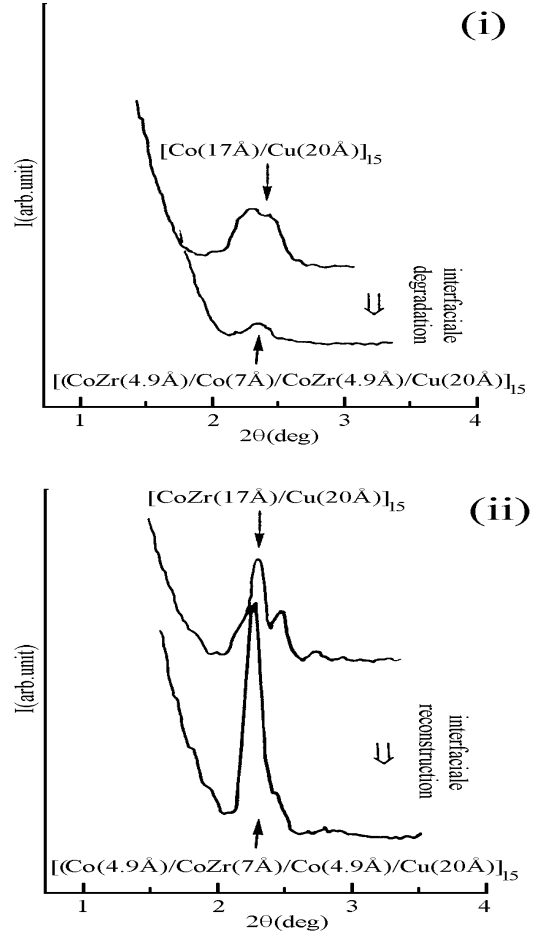


FIG. 4 : X-ray diffraction spectra at low angles. Influence of interfacial insertions of CoZr and Co films in $[\text{Co}(7\text{\AA})/\text{Cu}(20\text{\AA})]_{15}$ and $[\text{CoZr}(7\text{\AA})/\text{Cu}(20\text{\AA})]_{15}$ multilayers.

These spectra show that the insertion of a thin CoZr film in interfaces of (Co/Cu) multilayers reduces the Bragg line intensity, thus confirming the increase of the interfacial disorder (figure 4i). Whereas the insertion of a Co film with the same thickness in (CoZr/Cu) interfaces enhances the Bragg line intensity, thus favoring an interfaces reconstruction (figure 4ii).

C. MR AND ρ_s BEHAVIOR VERSUS P_{Cu}

Figure 5 shows the experimental evolution at $T=300\text{K}$ of the MR and ρ_s versus t_{Cu} for various P_{Cu} in the $[\text{Co}_{98}\text{Zr}_2 (25\text{\AA})/\text{Cu} (t_{\text{Cu}})/\text{Co} (25\text{\AA})]$ magnetic sandwiches. The MR curves exhibit a maximum which increases and moves towards larger t_{Cu} for increasing P_{Cu} (figure 5i). The saturation resistivity ρ_s decreases with increasing t_{Cu} while it increases with increasing P_{Cu} (figure 5ii). This MR and ρ_s behavior may be a result of variations of the interfacial structural quality and electronic scattering across this interface.

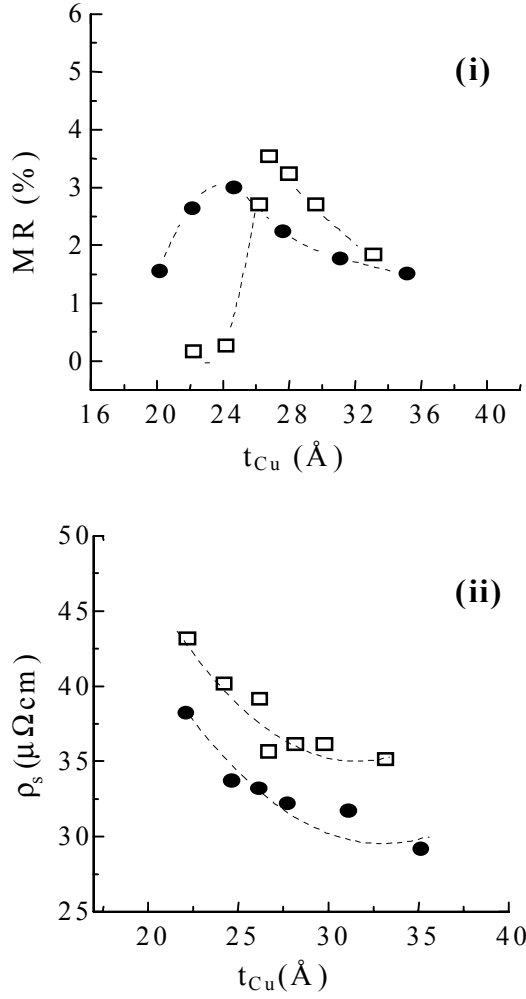


FIG. 5 : MR (i) and ρ_s (ii) measured at $T=300\text{K}$ in $[\text{Co}_{98}\text{Zr}_2 (25\text{\AA})/\text{Cu} (t_{Cu})/\text{Co} (25\text{\AA})]$ magnetic sandwiches versus t_{Cu} for different P_{Cu} . Solid circles: $P_{Cu}=0.5 \times 10^{-2}$ mbar; open squares: $P_{Cu}=1.2 \times 10^{-2}$ mbar; dashed lines are guide for eyes.

Next, we will treat the P_{Cu} effect on the magnetoresistive properties of the $[\text{Co}_{98}\text{Zr}_2 (25\text{\AA})/\text{Cu} (t_{Cu})/\text{Co} (25\text{\AA})]$ magnetic sandwiches using the semi-classical approach based on the Johnson-Camley model¹² that we have already applied in the $[\text{Co}_{98}\text{Zr}_2(t_{CoZr})/\text{Cu}(28\text{\AA})/\text{Co}(25\text{\AA})]$ sandwiches to account for the t_{CoZr} effect on MR and ρ_s of this system⁸.

IV. DISCUSSION

A. t_{CoZr} EFFECT ON THE MR

In a previous work realized on the $[\text{Co}_{98}\text{Zr}_2 (t_{CoZr})/\text{Cu} (28\text{\AA})/\text{Co} (25\text{\AA})]$ magnetic sandwiches with 2 Zr at% in Co, the study of the t_{CoZr} effect on the magnetoresistive properties allowed us to point out the existence of a disordered phase "CoZrCu" of thickness $t_{\text{alloy}} \approx A t_{CoZr}$

at the CoZr/Cu interface, where A is an adjustable parameter⁸. The widening of the disordered phase characterizes non homogeneous and rougher interfaces. The Cu, CoZr and Co deposition pressures have been fixed respectively at 1.2×10^{-2} mbar, 2×10^{-3} mbar and 5×10^{-2} mbar (table 1). A very satisfactory agreement, simultaneously for the MR and ρ_s , between experiments and calculations has been obtained for a parameter A equal to 0.04 (figure 6). The other parameters of the calculations were fixed as in table 2. The significant result of the simulation, confirmed experimentally, is the increase of ρ_s with increasing disordered phase thickness or concentration reflected by an increase of the parameter A (figure 6ii). In contrast, the MR magnitude decreases more and more when the interfacial disorder concentration becomes dominant (figure 6i), thus reflecting a deterioration of the interfacial quality.

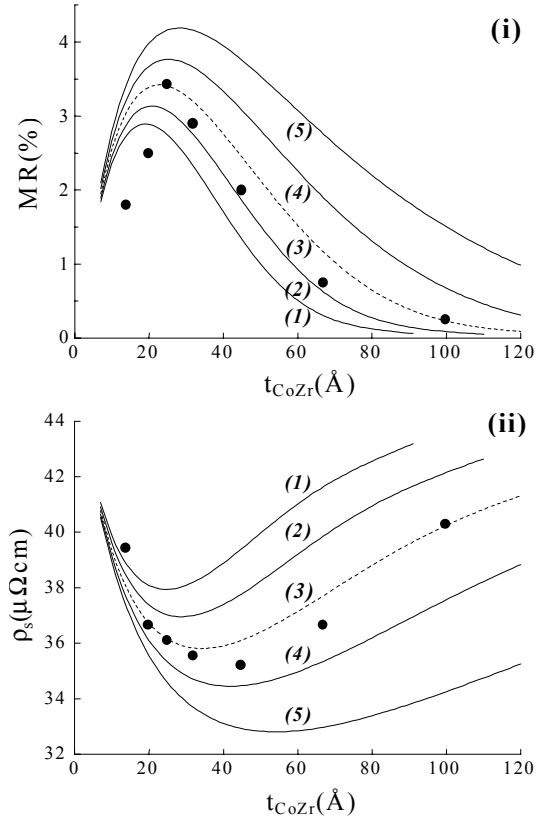


FIG. 6 : Variation of the MR (i) and ρ_s (ii) in the $[\text{Co}_{98}\text{Zr}_2 (t_{CoZr})/\text{Cu} (28\text{\AA})/\text{Co} (25\text{\AA})]$ magnetic sandwiches versus t_{CoZr} for $P_{Cu}=1.2 \times 10^{-2}$ mbar⁸.

The other parameters are fixed (tables 1 and 2). Solid circles: Experimental results at $T=300\text{K}$; lines: Set of fits of experimental data for different values of the parameter A . (1): $A=0.06$; (2): $A=0.05$; (3): $A=0.04$; (4): $A=0.03$; (5): $A=0.02$; dashed lines are calculations agree well with experiment.

Tab. 1: Experimental resistivities of CoZr, Cu and Co layers measured at room temperature for different pressures. The corresponding electronic MFP are deduced from the relation: $\rho\lambda=970$, where $\rho(\mu\Omega\text{cm})$ and $\lambda(\text{\AA})$ are the mean values of the resistivity and the electronic MFP²⁰.

| Layer | Pressure (mbar) | Resistivity ($\mu\Omega\text{cm}$) | MFP (\AA) |
|-------|----------------------|--------------------------------------|----------------------|
| CoZr | 2×10^{-3} | 38 | 26 |
| Cu | 0.5×10^{-2} | 5 | 194 |
| | 1.2×10^{-2} | 6 | 162 |
| Co | 5×10^{-2} | 45 | 22 |

Tab. 2: Calculation parameters. α_{CoZr} and α_{Co} are SDSA coefficients in CoZr and Co layers; t_{mx} is the mixed zone thickness; \hat{a}_{mx}^0 and \hat{e}_{mx}^0 are the SDSA coefficient and the electronic MFP in the mixed zone without disordered phase; \hat{a}_{alloy} is the SDSA coefficient of the alloying phase "CoZrCu" which diffuse into the magnetic CoZr layer.

| \hat{a}_{CoZr} | \hat{a}_{Co} | $t_{\text{mx}} (\text{\AA})$ | \hat{a}_{mx}^0 | $\hat{e}_{\text{mx}}^0 (\text{\AA})$ | \hat{a}_{alloy} |
|-------------------------|-----------------------|------------------------------|-------------------------|--------------------------------------|--------------------------|
| 2 | 5 | 6 | 10 | 10 | 2 |

B. P_{Cu} EFFECT ON THE MR

a- P_{Cu} INFLUENCE ON THE DISORDERED PHASE CONCENTRATION: $A=A(P_{\text{Cu}})$

In this part, we analyze the MR and ρ_s experimental results measured at $T=300\text{K}$ versus t_{Cu} in the $[\text{Co}_{98}\text{Zr}_2(25\text{\AA})/\text{Cu}(t_{\text{Cu}})/\text{Co}(25\text{\AA})]$ magnetic sandwiches for various P_{Cu} , using the previous model⁸. When P_{Cu} varies, the interfacial quality CoZr/Cu and thereafter the disordered phase "CoZrCu" concentration will be directly affected. Thus, the study of the P_{Cu} effect on the magnetoresistive properties can be described by the change in the alloying phase "CoZrCu" concentration. Indeed, the alloying phase effect can simply be represented by a chemical pressure exerted on the interfaces. Using the same model⁸ with identical parameters (tables 1 and 2), we aim at determining the appropriate A values that lead to a good agreement between experiment and calculations. Taking into account the Cu resistivity variation from one pressure to another, we have tried first to reproduce measured ρ_s versus t_{Cu} for each pressure under investigation. Figure 7ii represents the fit of the $\rho_s(t_{\text{Cu}})$ evolution for the two Cu pressures. A satisfactory agreement with experiments is obtained for values of $A \approx 0$ and $A = 0.04$, which correspond respectively to Cu deposition pressures of 0.5×10^{-2} mbar and 1.2×10^{-2} mbar.

This marks the importance of the P_{Cu} effect on the alloying phase concentration.

Using the same fit parameters for calculating the MR shape as a function of t_{Cu} for each pressure, we obtain a qualitative agreement with experimental results for $P_{\text{Cu}} = 1.2 \times 10^{-2}$ mbar (figure 7i, curve 1). This confirms the t_{CoZr} effect on MR and ρ_s in the $[\text{Co}_{98}\text{Zr}_2 (t_{\text{CoZr}})/\text{Cu} (28\text{\AA})/\text{Co} (25\text{\AA})]$ magnetic sandwiches.

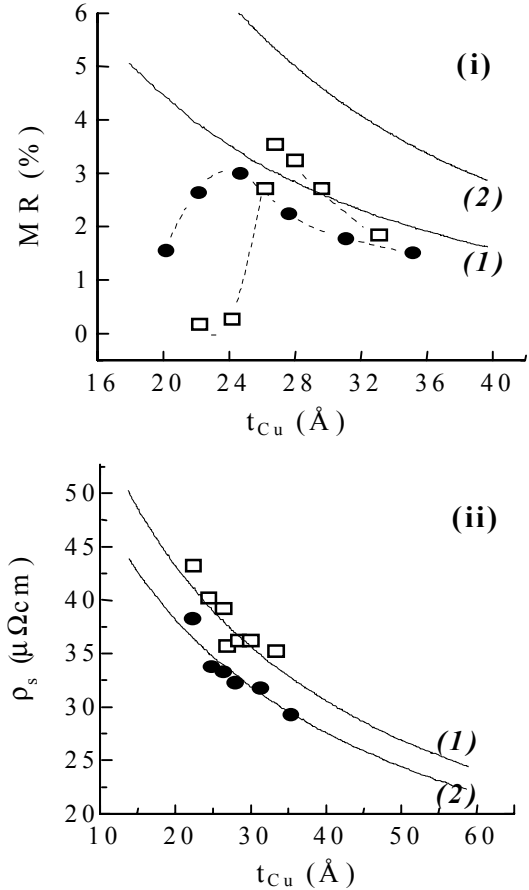


FIG. 7 : MR (i) and ρ_s (ii) evolution as a function of t_{Cu} for different Cu deposition pressures in $[\text{Co}_{98}\text{Zr}_2 (25\text{\AA})/\text{Cu} (t_{\text{Cu}})/\text{Co} (25\text{\AA})]$ magnetic sandwiches. Dashed lines are guide for eyes; lines represent the fit of experimental data; (\bullet , (2)): $P_{\text{Cu}} = 0.5 \times 10^{-2}$ mbar; (\square , (1)): $P_{\text{Cu}} = 1.2 \times 10^{-2}$ mbar.

However, for $P_{\text{Cu}} = 0.5 \times 10^{-2}$ mbar, there are some discrepancies between measured and calculated magnetoresistances (MR_{exp} and MR_{cal}) (figure 7i, curve 2). These discrepancies suggest that the MR is, in addition to the alloying phase effect treated above, more sensitive to the P_{Cu} effect through the other interfacial parameters such as the electronic MFP \hat{e}_{mx}^0 , SDSA coefficient \hat{a}_{mx}^0 and the mixed zone thickness t_{mx} . These parameters can then be considered as P_{Cu} dependent, i.e.: $\hat{e}_{\text{mx}}^0 = \hat{e}_{\text{mx}}^0(P_{\text{Cu}})$, $\hat{a}_{\text{mx}}^0 = \hat{a}_{\text{mx}}^0(P_{\text{Cu}})$ and $t_{\text{mx}} = t_{\text{mx}}(P_{\text{Cu}})$. Thus, the P_{Cu} effect on the MR can be treated indirectly through a study of the influence of these parameters.

b. P_{Cu} INFLUENCE ON THE INTERFACIAL PARAMETERS:

$$\mathcal{E}_{mx}^0 = \mathcal{E}_{mx}^0(P_{Cu}), \quad \hat{a}_{mx}^0 = \hat{a}_{mx}^0(P_{Cu}) \quad \text{AND} \quad t_{mx} = t_{mx}(P_{Cu})$$

In order to more define the impact of the parameters \mathcal{E}_{mx}^0 , \hat{a}_{mx}^0 and t_{mx} , we fixed P_{Cu} and followed the MR_{cal} evolution with t_{Cu} for each of these parameters (figures 8i, ii and iii). The rapid decrease of the MR with t_{Cu} presents an almost universal aspect for any value of the parameters \mathcal{E}_{mx}^0 and \hat{a}_{mx}^0 (figures 8i and ii). This reveals that \mathcal{E}_{mx}^0 and \hat{a}_{mx}^0 have not a great influence on MR, as it preserves an identical shape for different values of these parameters, but still remains far from experimental results (figure 5i). In contrast, when changing t_{mx} , the MR_{cal} magnitude varies significantly and becomes closer to the experimental results (figure 8iii).

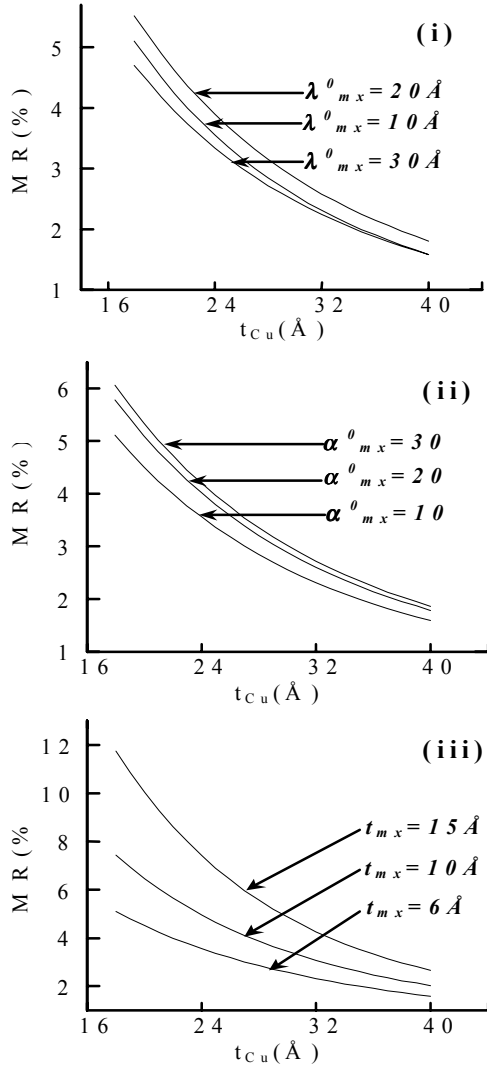


FIG. 8: Calculated MR evolution as a function of the Cu layer thickness deposited at $P_{Cu} = 1.2 \times 10^{-2}$ mbar in the $[Co_{98}Zr_2 (25\text{\AA})/Cu (t_{Cu})/Co (25\text{\AA})]$ magnetic sandwiches for different values of \mathcal{E}_{mx}^0 (i), \hat{a}_{mx}^0 (ii) and t_{mx} (iii).

Consequently, in addition to the alloying phase effect represented by the parameter A, it is the variation of the mixed zone thickness t_{mx} which represents better the P_{Cu} effect on the MR behavior. Thus, the MR evolution can be analyzed as a function of two parameters P_{Cu} -dependent: $A = A(P_{Cu})$ and $t_{mx} = t_{mx}(P_{Cu})$.

c. MR EVOLUTION WITH $A(P_{Cu})$ AND $t_{mx}(P_{Cu})$

In order to reproduce simultaneously experimental values of MR and ρ_s , we have varied both the parameter A and the mixed zone thickness t_{mx} . Results are shown on figures 9i and ii. The optimal parameters deduced from the best fit are summarized in table 3.

Tab. 3: Optimal values of the parameters A and t_{mx} deduced from the best fit of the MR and ρ_s .

| $P_{Cu} (\times 10^{-2} \text{ mbar})$ | Parameters | |
|--|------------|-----------------------|
| | A | $t_{mx} (\text{\AA})$ |
| 0.5 | 0.02 | 2 |
| 1.2 | 0.04 | 6 |

The agreement obtained between experimental and calculated MR is more than satisfactory, suggesting that the P_{Cu} effect is essentially reproduced by a simultaneous variation of the alloying phase concentration "CoZrCu" and the thickness t_{mx} of the interfacial mixed zone containing this alloy.

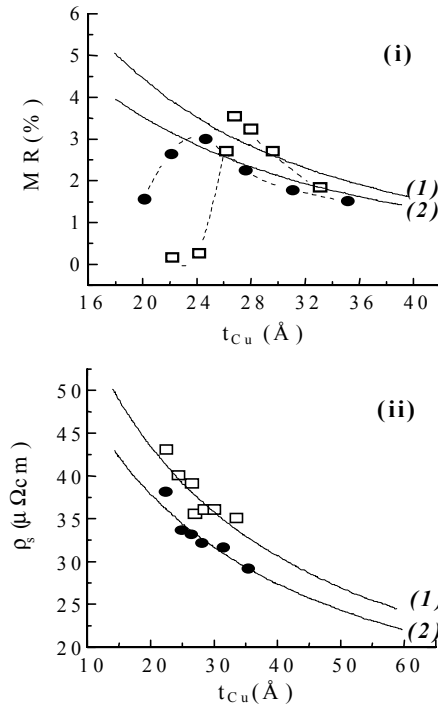


FIG. 9: MR (i) and ρ_s (ii) variation in the $[Co_{98}Zr_2 (25\text{\AA})/Cu (t_{Cu})/Co (25\text{\AA})]$ magnetic sandwiches versus t_{Cu} for the optimal values of the parameters A and t_{mx} summarized in the table 3. Dashed lines are guide for eyes; lines denote the fit; (\bullet , (2)): $P_{Cu} = 0.5 \times 10^{-2}$ mbar; (\square , (1)): $P_{Cu} = 1.2 \times 10^{-2}$ mbar.

The mixed zone widening with increasing P_{Cu} can be explained by the fact that when the pressure increases, the probability of non magnetic Cu atoms scattering within the CoZr and Co magnetic layers becomes more important. Thus, the more increase in t_{mx} , the more significant the bulk effect on the MR becomes. Indeed, going from a thin interface ($t_{\text{mx}}=2\text{\AA}$) to a mixed zone ($t_{\text{mx}}=6\text{\AA}$), the electronic spin-dependent scattering in the CoZr magnetic layer changes from the interfacial (MR^{max} for small values of t_{Cu}) to a bulk nature (MR^{max} moves towards large values of t_{Cu}), which is in good agreement with the previous results^{21,22}. Consequently, the experimentally observed MR maximum shift-over to large Cu thicknesses when P_{Cu} increases, may be essentially due to the increase of the mixed zone thickness parameter t_{mx} . Furthermore, the increase of P_{Cu}

favors the "CoZrCu" disordered phase, thus giving rise to an increase of ρ_{S} .

V. CONCLUSION

The results of the P_{Cu} effects on the magnetoresistive properties are discussed in the framework of the Johnson-Camley semi-classical model. The strikingly good agreement between experimental and calculated MR and ρ_{S} may convey that the increase in P_{Cu} essentially results in a reinforcement of the "CoZrCu" disordered phase inside the mixed zone, whose thickness t_{mx} can also be enlarged by the increase of the P_{Cu} parameter.

¹ M. N. Baibich, J. M. Broto, A. Fert, F. Nguyen Van Dau, F. Petroff, P. Etienne, G. Creuzet, A. Friederich and J. Chazelas, *Phys. Rev. Lett.* **61** (1988) 2472.

² D. Mosca, F. Petroff, A. Fert, P. A. Schroeder, W. P. Pratt Jr. and R. Laloe, *J. Magn. Magn. Mat.* **94** (1991) L1.

³ M. B. Stearns, Y. Cheng and C. H. Lee, *J. Appl. Phys.* **67** (1990) 5925.

⁴ F. Petroff, A. Barthèlèmy, D. H. Mosca, D. K. Lottis, A. Fert, P. A. Schroeder, W. P. Pratt Jr., R. Laloe and S. Lequien, *Phys. Rev. B* **44** (1991) 5355.

⁵ R. E. Camley and J. Barnas, *Phys. Rev. Lett.* **63** (1989) 664.

⁶ D. M. Edwards, J. Mathon and R. B. Muniz, *IEEE Trans. Magn.* **27** (1991) 3548.

⁷ P. M. Levy, S. Zhang and A. Fert, *Phys. Rev. Lett.* **65** (1990) 1643.

⁸ M. Faris, M. El Harfaoui, A. Qachaou, J. Ben Youssef, H. Le Gall and D. Meziane Mtalsi, *M. J. Cond. Mater.* **2/1** (1999) 1; M. El Harfaoui, M. Faris, A. Qachaou, J. Ben Youssef, H. Le Gall and D. Meziane Mtalsi, *J. Magn. Magn. Mater.* **223/1** (2000) 81.

⁹ S. Zhang and P. M. Levy, *Phys. Rev. B* **43** (1991) 11048.

¹⁰ F. Petroff, A. Barthèlèmy, A. Hamzic, A. Fert, P. Etienne, S. Lequien and G. Creuzet, *J. Magn. Magn. Mater.* **93** (1991) 95.

¹¹ S. Zhang and P. M. Levy, *Mat. Res. Soc. Symp. Proc. Spring* (1991).

¹² B. L. Johnson and R. E. Camley, *Phys. Rev. B* **44** (1991) 9997.

¹³ T. Shinjo and H. Yamamoto, *J. Phys. Soc. Jpn.* **59** (1990) 3061.

¹⁴ M. Jimbo, T. Kanda, S. Goto, S. Tsunashima and S. Uchiyama, *J. Magn. Magn. Mater.* **126** (1993) 422.

¹⁵ S. Gangopadhyay, S. Hossain, J. Yang, J. A. Barnard, M. T. Kief, H. Fujiwara and M. R. Parker, *J. Appl. Phys.* **76** (1994) 6522.

¹⁶ M. Jimbo, K. Komiyama, H. Matsue, S. Tsunashima and S. Uchiyama, *J. Appl. Phys.* **34** (1995) L112.

¹⁷ M. A. Akhter, Y. Q. Matan and D. J. Mapps, *MMM, Conf. Atlanta Nov* (1996) BR-11.

¹⁸ J. Ben Youssef, H. Le Gall, K. Bouziane, M. El Harfaoui, O. Koshkina, J. M. Desvignes et A. Fert, *Journal de Physique IV* **6** (1996) 161; J. Ben Youssef, K. Bouziane, O. Koshkina, H. Le Gall, M. El Harfaoui, M. El Yamani, J. M. Desvignes and A. Fert, *J. Magn. Magn. Mater.* **165** (1997) 288.

¹⁹ J. Langer, *The CAMST RECORD, Read-write* **28** (1996) 35.

²⁰ J. L. Duvail, A. Fert, L. G. Pereira and D. K. Lottis, *J. Appl. Phys.* **75** (1994) 7070.

²¹ J. Barnas, A. Fuss, R. E. Camley, P. Grünberg and W. Zinn, *Phys. Rev. B* **42** (1990) 8110.

²² B. Dieny, *J. Phys. Cond. Mat.* **4** (1992) 8009.